CILAMCE 2017
Florianópolis - Santa Catarina - Brazil

HIGH-ORDER METHODS FOR THE ACOUSTIC WAVE EQUATION IN ONE SPACE DIMENSION

Juliano Deividy B. Santos

Abimael Fernando D. Loula

juliano@lncc.br

aloc@lncc.br

Laboratório Nacional de Computação Científica, LNCC

Getúlio Vargas Av., 333, Quitandinha Petrópolis - Rio de Janeiro CEP 25651-075 - Brasil

Abstract. *Finite difference methodologies are classically generated by Taylor series expansions. In this work we present a methodology to obtain finite difference approximations of different orders for the acoustic wave equation in one space dimension, aiming at obtaining high order methods compared to the classical ones. Unlike the usual methodologies, we will use polynomial basis functions in space and time to obtain the stencil coefficients (compact or not). To this end, bases of characteristic polynomials are used to obtain the coefficients. For stencils with seven and nine points and the time step of the same order as the spatial step, higher order methods are obtained compared to the classical methodologies. A stability analysis is performed showing that the stability conditions for the proposed methodology are less restrictive than those corresponding to the classical finite difference discretizations. Numerical experiments are conducted, corroborating the predicted orders of convergence analysis.*

Keywords: *Finite Differences, Acoustic wave equation, Characteristic polynomials.*

1 ONE-DIMENSIONAL MODEL PROBLEM

Consider a vibrating string with fixed ends in a domain $\Omega = [0, L]$ and let $u(x, t)$ be a function that denotes the vertical displacement of the string at the point x and time t. Since the wave equation is second order in the derivatives, its initial conditions will be described as position and initial velocity. The initial value problem in the variable t of boundary values in the associated variable x will is

$$\begin{aligned} &\frac{\partial^2 u}{\partial t^2} - c^2\frac{\partial^2 u}{\partial x^2} = 0,\ \ 0 < x < L,\ \ t > 0, \\ &u(0,t) \ = \ u(L,t) = 0,\ \ t \geq 0 \\ &u(x,0) = f(x),\ \frac{\partial u(x,0)}{\partial t} = h(x),\ \ 0 \leq x \leq t. \end{aligned} \tag{1}$$

The figure 1 shows an illustration of the problem 1.

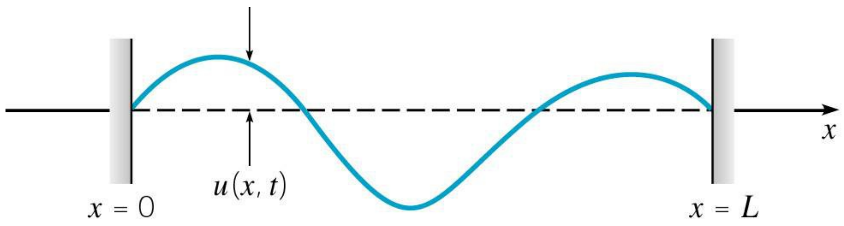

Figure 1: Example of a vibrant string with fixed ends in a domain $\Omega = [0, L]$

By discretizing the domain $\Omega \subset \mathbb{R}$ discretized using $N + 1$ points equidistant in space/time

$$x_j := jh, j = 0, 1, \ldots, N,$$

$$t_n := n\Delta t, n = 0, 1, \ldots, M$$

where $h = \frac{1}{N}$, and the steps in space and time given by $h := x_{j+1} - x_j$ e $\Delta t := t_{n+1} - t_n$, respectively. We will denote an approximation $u(x, t)$ at the time level t_n in the position x_j by

$$U_j^n \approx u(x_j, t_n). \tag{2}$$

It is well known that the terms

$$D_{tt}U_j^n = \frac{U_j^{n+1} - 2U_j^n + U_j^{n-1}}{\Delta t^2} = \frac{\partial u(x_j, t_n)}{\partial t^2} + O(\Delta t^2), \tag{3}$$

$$D_{xx}U_j^n = \frac{U_{j+1}^n - 2U_j^n + U_{j-1}^n}{h^2} = \frac{\partial u(x_j, t_n)}{\partial x^2} + O(h^2) \tag{4}$$

approximate the second derivatives in time and space of a sufficiently regular function $u(x, t)$, that is, $u \in C^{4,4}(0, L) \times (0, T)$, at the point $x_j = jh$ and $t_n = n\Delta t$, with an error of the order of h^2 and Δt^2, respectively. Consequently the equation of differences

$$D_{tt}U_j^n - c^2 D_{xx}U_j^n = 0, \tag{5}$$

which is expressed explicitly and normalized as

$$U_j^{n+1} + 2\left(\frac{c^2\Delta t^2}{h^2} - 1\right)U_j^n - \frac{c^2\Delta t^2}{h^2}U_{j+1}^n + \frac{c^2\Delta t^2}{h^2}U_{j-1}^n + U_j^{n-1} = 0, \tag{6}$$

and approaches the one-dimensional model problem 1 with a truncation error

$$\tau_j^n = O(h^2, \Delta t^2). \tag{7}$$

The Figure 2 is a five-point stencil that relates U_j^n to its 4 neighbor nodes.

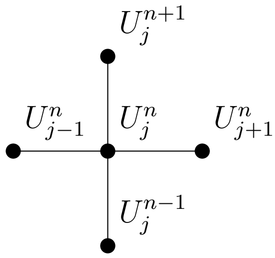

Figure 2: Uniform Stencil of 5 points for an approximation of second order finite differences in time and space

In the next section, we will introduce a methodology to obtain different stencils, where we will see that the coefficients of the stencil will characterize each approach.

2 APPROXIMATIONS OF DIFFERENT SPATIAL ORDERS

To obtain the finite difference coefficients to be used in numerical experiments we will proceed in accordance with the approach presented in [1]; [2]; [3]. For this, we will consider Ω a limited open domain. By means of differential operators, a problem with boundary values can be abstractly as:

Problem: Find field variables $\mathbf{u}(\mathbf{x})$: $\Omega \longrightarrow \mathbb{R}$, $\forall \mathbf{x} \in \Omega$, such that

$$\mathcal{L}(\mathbf{u}) \;=\; \mathbf{f} \qquad \text{em } \Omega, \tag{8}$$

with the boundary conditions given by:

$$\mathcal{B}(\mathbf{u}) \;=\; \bar{\mathbf{g}} \qquad \text{sobre } \Gamma \tag{9}$$

Where $\mathbf{f}$ is a source term defined in domain Ω and $\bar{\mathbf{g}}$ is the prescribed boundary condition on the entire contour Γ. The operators $\mathcal{L}$ and $\mathcal{B}$ represent a system of partial differential equations in the domain Ω and in the contour Γ, respectively.

The discretization of equations (8) and (9) can be described in such a way that it is independent of the number of points used in the stencil.

Considering that the equation (8) is a partial differential equation of a scalar variable $u(\mathbf{x})$, $\mathbf{x} \in \Omega \subset \mathbb{R}^2$, its classical approximation in finite differences over a point $x_i \in \mathcal{I}$ must meet the following relation

$$\mathcal{L}u(\mathbf{x}_i) \cong \sum_{j \in \mathcal{A}_i} c_j u(\mathbf{x}_j), \tag{10}$$

with the coefficients c_j, with $j \in \mathcal{A}_i$, calculated in such a way that the value of the operator $\mathcal{L}$ on the variable u at point $\mathbf{x}_I$ is given as a linear combination of the value of the function u evaluated at the points $\mathbf{x}_j$ belonging to a neighborhood $\mathcal{A}_i$ of $\mathbf{x}_i$.

The mesh pitch h can have its set of mapped points by $x_i = x_0 \pm ih\ i = 1, 2, \ldots$. We adopt the nomenclature U_j as a possible approach $u(x_j)$, at node j, where U_j is prescribed if $x_j \in \mathcal{B}$.

The approximation of the operator in its strong form can be replaced by its version in discrete form, having the advantage of reducing the order of the approximate derivatives.

The calculation of c_j, finite difference stencil in $\mathbf{x}_i$, can be realized in several ways. Here we will use the direct expression given by the equation (10), substituting the variable u for each of the $|\mathcal{A}_i|$ basis functions $\mathbb{B}_i$ evaluated at the point $\mathbf{x}_i$. Using a base $\mathbb{B}_i$ with m functions φ_j,

$$\mathbb{B}_i := \{\varphi_1, \varphi_2, \ldots, \varphi_{|\mathcal{A}_i|}\}, \tag{11}$$

we get for every φ_l, $l = 1, \ldots, |\mathcal{A}_i|$, an equation,

$$\sum_{j \in \mathcal{A}_i} c_j \varphi_l(\mathbf{x}_j) = \mathcal{L}\varphi_l(\mathbf{x}_i), \tag{12}$$

which is evaluated at point i, resulting in a system of $|\mathcal{A}_i|$ linear algebraic equations. In matrix form, with $m = |\mathcal{A}_i|$, such a system is given by

$$\underbrace{\begin{bmatrix} \gamma_{11} & \gamma_{12} & \gamma_{13} & \cdots & \gamma_{1m} \\ \gamma_{21} & \gamma_{22} & \gamma_{23} & \cdots & \gamma_{2m} \\ \vdots & \vdots & \vdots & \ddots & \vdots \\ \gamma_{m1} & \gamma_{m2} & \gamma_{m3} & \cdots & \gamma_{mm} \end{bmatrix}}_{\Gamma} \underbrace{\begin{bmatrix} c_1 \\ c_2 \\ \vdots \\ c_m \end{bmatrix}}_{C} = \underbrace{\begin{bmatrix} f_1 \\ f_2 \\ \vdots \\ f_m \end{bmatrix}}_{F} \tag{13}$$

where Γ is the input matrix $\gamma_{lj} = \varphi_l(\mathbf{x}_j)$, $j, l = 1...k$, C is the vector of unknowns and F is the source term vector with components $f_l = \mathcal{L}\varphi_l \mathbf{x}i$. The $|\mathcal{A}_i|$ points $\mathbf{x}_j$ are chosen according to a criterion to ensure that the matrix Γ is not singular and to obtain the best representation of the operator by the stencil of differences.

The finite difference approximations will be obtained by applying the polynomial function bases methodology in x and t on stencils of 5, 7 and 9 points corresponding to second, fourth and sixth order approximations in space respectively and second order in time as shown in the Figure 3. To obtain the coefficients that characterize a classical approximation of finite differences we will use the canonical polynomials that constitute the bases

$$\mathbb{B}_5 := \{1, t, t^2, x, x^2\}, \tag{14}$$

$$\mathbb{B}_7 := \{1, t, t^2, x, x^2, x^4, x^5\} \tag{15}$$

e

$$\mathbb{B}_9 := \{1, t, t^2, x, x^2, x^4, x^5, x^6, x^7\},$$

employed in the methodology.

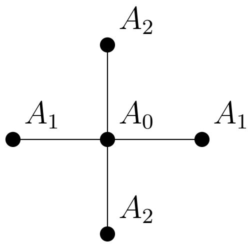

(a) Stencil of 5 points.

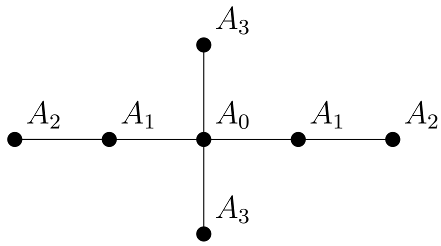

(b) Stencil of 7 points.

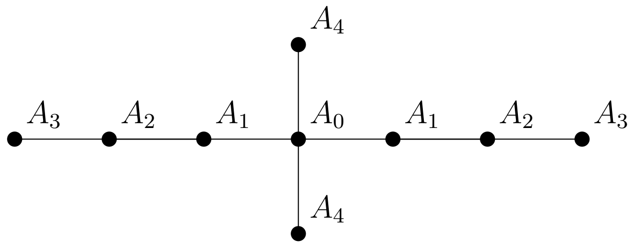

(c) Stencil of 9 points.

Figure 3: Stencils of different orders.

For example, to obtain the second-order finite difference approximation in space and time (5) we consider the set

$$\mathbb{B}_5 := \{1, t, t^2, x, x^2\}, \tag{16}$$

associated with the five points illustrated in Figure 4, where each polynomial is denoted by $p_j(x, t)$, $j = 1, 2, \ldots, 5$.

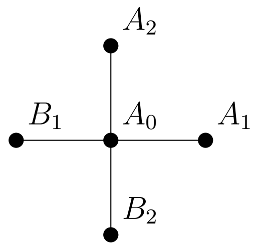

Figure 4: Uniform Stencil of 5 points for the finite difference scheme of second order in time and space

For the assembly of the associated system of equations, we evaluate each polynomial $p_j \in \mathbb{B}_5$ on the nodes of the stencil by applying them to the operator

$$\mathcal{L}[\,] = \frac{\partial^2}{\partial t} - c^2 \frac{\partial^2}{\partial x^2}. \tag{17}$$

In this way we obtain the following equations for the determination of the coefficients of the stencil:

1) For $p_1(x, t) = 1 \Rightarrow A_1 + A_0 + B_1 + A_2 + B_2 = \mathcal{L}[p_1] = 0$.
2) For $p_2(x, t) = t \Rightarrow -A_2 \Delta t + B_2 \Delta t = \mathcal{L}[p_2] = 0$.

3) For $p_3(x,t) = x \Rightarrow -A_1 h + B_1 h = \mathcal{L}[p_3] = 0$.
4) For $p_4(x,t) = t^2 \Rightarrow A_2 \Delta t^2 + B_2 \Delta t^2 = \mathcal{L}[p_4] = 2$.
5) For the polynomial $p_5(x,t) = x^2 \Rightarrow A_1 h^2 + B_1 h^2 = \mathcal{L}[p_5] = -2c^2$.

Solving the system of the five equations obtained previously yield

$$\begin{aligned} &B_1 = A_1,\ B_2 = A_2 \\ &A_1 = -\frac{c^2}{h^2},\ A_2 = \frac{1}{\Delta t^2}, \\ &A_0 = -2A_1 - 2A_2 = \left(\frac{2}{\Delta t^2} - \frac{2c^2}{h^2}\right). \end{aligned} \tag{18}$$

Classically we obtain the same coefficients of the stencil associated with equation (6). Consistently, the approximation orders of the proposed finite difference methods will be characterized, always assuming sufficiently regular solutions, using characteristic polynomials satisfying this equation.

3 GENERATION OF STENCILS VIA CHARACTERISTIC CURVES

It is known that the general solution of the homogeneous wave equation in one space dimension is given by

$$u(x,t) = f(x+ct) + g(x-ct), \tag{19}$$

where $f, g \in C^2(\mathbb{R})$ are arbitrary functions. We propose new approaches in which sets $\mathbb{C}_j$ are formed by characteristic polynomials, written in terms of characteristic curves. To obtain the coefficients for a five-point stencil, we use the base:

$$\mathbb{C}_1 := 1, (x-ct), (x+ct), x^2, (x+ct)^2, \tag{20}$$

which when used in the method described in the previous section gives us the classical coefficients:

$$A_0 := 1 - \mu^2,\ A_1 := \mu^2,\ A_2 := 1; \tag{21}$$

because $\mathbb{C}_1$ and $\mathbb{B}_5$ are linearly independents.

For the seven-point stencil the base set shall be the next:

$$\mathbb{C}_2 := \{1, (x-ct), x^2, (x+ct)^2, (x-ct)^3, (x+ct)^4, (x-ct)^5\}, \tag{22}$$

with the associated approximation will be explicitly given by with

$$A_3 U_j^{n+1} + A_2 U_{j+2}^n - A_1 U_{j+1}^n + A_0 U_j^n - A_1 U_{j-1}^n + A_2 U_{j-2}^n + A_3 U_j^{n-1} = 0 \tag{23}$$

where the associated coefficients

$$A_0 := -\frac{\mu^4}{2} + \frac{5}{2}\mu^2 - 2,\ A_1 := \frac{\mu^4 - 4\mu^2}{3}\mu^2$$
$$A_2 := -\frac{\mu^4 - \mu^2}{12},\ A_3 := 1$$

where $\mu = \dfrac{\Delta t \cdot c}{h}$.

Next, to obtain the coefficients associated with the nine-point stencil, the following base set will be considered

$$\mathbb{C}_3 := \{1, (x-ct), x^2, (x+ct)^2, (x-ct)^3, (x+ct)^4, (x-ct)^5, (x+ct)^6, (x-ct)^7\}. \quad (24)$$

In fact, the approximate explicit form will be

$$A_4 U_j^{n+1} - A_3 U_{j+3}^n + A_2 U_{j+2}^{n+1} - A_1 U_{j+1}^n + A_0 U_j^n - A_1 U_{j-1}^n + A_2 U_{j-2}^n - A_3 U_{j-3}^n A_4 U_j^{n-1} = 0 \quad (25)$$

with

$$A_0 := \frac{\mu^6 + 49\mu^2}{18} - \frac{7}{9}\mu^4 - 2,\ A_1 := -\frac{\mu^6 - 13\mu^4 + 36\mu^2}{24}$$
$$A_2 := \frac{\mu^6 - 10\mu^4 + 9\mu^2}{60},\ A_3 := -\frac{\mu^6 - 5\mu^4 + 4\mu^2}{360}, \quad .$$
$$A_4 := 1$$

3.1 Order of convergence

The truncation error will characterize the order of each approximation. Thus, the order of approximation of the finite difference method (5) will be determined using the polynomials

$$\varphi_k(x - ct) = (x - ct)^k \quad (26)$$

and

$$\psi_k(x + ct) = (x + ct)^k \quad (27)$$

with $x \in [-h, h]$ e $t \in [-\Delta t, \Delta t]$.

We note that, for $k = 0, 1, 2$

$$D_{tt}\varphi_k(x_j, t_n) - c^2 D_{xx}\varphi_k(x_j, t_n) = 0,\ k = 0, 1, 2, \quad (28)$$

$$D_{tt}\psi_k(x_j, t_n) - c^2 D_{xx}\psi_k(x_j, t_n) = 0,\ k = 0, 1, 2, \quad (29)$$

by the construction of the methods.

For $k \geq 3$, given the symmetry of the stencil, we have

$$D_{tt}\varphi_k(x_j, t_n) - c^2 D_{xx}\varphi_k(x_j, t_n) = \tau_k(\Delta t, h). \quad (30)$$

$$D_{tt}\psi_k(x_j, t_n) - c^2 D_{xx}\psi_k(x_j, t_n) = \tau_k(\Delta t, h). \quad (31)$$

with

$$\tau_k(\Delta t, h) = c^2[(c\Delta t)^{k-2} + (-c\Delta t)^{k-2} - h^{k-2} - (-h)^{k-2}]. \quad (32)$$

From where we can conclude that:

1) For every k odd : $\tau_k(\Delta t, h) = 0$;
2) The order of approximation of this five-point stencil is characterized for $k = 4$, resulting: $\tau_4(\Delta t, h) = c^2[2c^2\Delta t^2 - 2h^2]$;
3) For $\Delta t = \dfrac{h}{c}$: $\tau_k(\Delta t, h) = 0,\ \forall\ k$,

meaning that for this choice $h = c\Delta t$, this method is nodally accurate.

The calculation of the truncation errors of the other approximations was performed by an analogous procedure. The Table (1) shows the order of convergence obtained for each stencil previously presented. Considering that the study is based on orthogonal Cartesian meshes, it is usual to take the step in time having the same order of step in space, that is, $\Delta t = O(h)$. Because of this classical approach, for all stencils, there was no gain of the order of spatial convergence, where second-order rates were obtained.

Stencil	**Convergence space / time**	**Convergence for $\Delta t = O(h)$**
5 points	$O(\Delta t^2, h^2)$	$O(h^2)$
7 points	$O(\Delta t^2, h^4)$	$O(h^2)$
9 points	$O(\Delta t^2, h^6)$	$O(h^2)$

Table 1: Convergence orders obtained for stencils of 5, 7 and 9 points, generated by polynomial bases composed of canonical polynomials. The last column doing $\Delta t = O(h)$.

The Table (2) presents the results obtained for the approximation orders of the stencils generated by characteristic polynomials. For the seven-point stencil, the approximation obtained was of the order $O(h^2 \cdot \Delta t^2, h^4)$. Therefore, for $\Delta t = O(h)$ this stencil generates a fourth-order approximation, unlike the seven points stencil obtained classically which is only second order. The nine-point stencil, on the other hand, achieved an even more expressive convergence gain. In fact, the order of convergence in the time-space was $O(h^4 \cdot\ \Delta t^2, h^6)$ so that for the step in time of the same order as the special step the method is $O(h^6)$.

Stencil	**Convergence space / time**	**Convergence for $\Delta t = O(h)$**
5 points	$O(\Delta t^2, h^2)$	$O(h^2)$
7 points	$O(\Delta t^2 \cdot h^2, h^4)$	$O(h^4)$
9 points	$O(\Delta t^2 \cdot h^4, h^6)$	$O(h^6)$

Table 2: Convergence orders obtained for stencils of 5, 7 and 9 points obtained by polynomial bases composed of characteristic polynomials. The last column making $\Delta t = O(h)$.

4 APPROACHES IN COMPACT STENCILS

Our methodology has shown results on uniform 9-point inner compact stencil meshes as given in Figure 5. Due to the symmetry, the coefficients to be determined are A_0, A_1, and A_2 associated with an implicit resolution of an associated linear system.

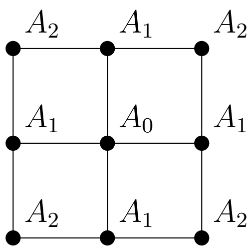

Figure 5: Compact stencil example of nine interior nodes of a uniform rectangular mesh.

Testing the approximation by means of the complete canonical polynomial base

$$\mathbb{B}_{3\times 3} = \{1, x, t, xt, x^2, t^2, x^2t, xt^2, x^2t^2\} \tag{33}$$

the same coefficients of the classic five-point stencil were obtained.

Now proceeding using the base of characteristic polynomials

$$\mathbb{C}_{3\times 3} = \{1, (x-ct), (x+ct), (x-ct)^2, (x)^2, (x-ct)^3, (x+ct)^3, (x-ct)^4, (x+ct)^4\} \tag{34}$$

the following coefficients characterized the approximation

$$A_0 = \frac{5\mu^2 - 5}{3},\ A_1 = -\frac{5\mu^2 + 1}{6},\ A_2 = -\frac{\mu^2 - 1}{12},$$

remembering that $\mu = \dfrac{\Delta t \cdot c}{h}$ and the truncation error given by

$$\tau_j^n = O(h^4, \Delta t^4), \tag{35}$$

therefore a fourth-order method in space and time. When we take $\Delta t = O(h)$ we have

$$\tau_j^n = O(h^4), \tag{36}$$

therefore a fourth-order method.

5 SPECTRAL STABILITY BY THE VON NEUMANN METHOD

For the stability analysis we use the method of von Neumann [4]; [5]; [6]. The analysis for the case of a nine-point stencil has not yet been concluded. Amount of terms involved. It is still in progress. The Table (3) presents a summary of the stability conditions for the 5, 7 and 9-point stencils with coefficients obtained classically and via characteristic polynomials.

Stencil	Stability to canonical polynomials	Stability to basis of characteristics
5 points	$\mu \leq 1$	$\mu \leq 1$
7 points	$\mu \leq \dfrac{\sqrt{3}}{2}$	$\mu \leq 1$
9 points	$\mu \leq \frac{3}{2}\sqrt{\frac{5}{17}}$	$\mu < 1$
9 points(compact)	$\mu \leq 1$	$\mu \leq 1$

Table 3: Table with stability conditions described for stencils of 5, 7 and 9 points.

As we can see, the stability conditions for the new approximations are less restrictive than the corresponding stability conditions of the classical methods.

6 COMPUTATIONAL EXPERIMENTS

6.1 Free Vibrations

In this section, we consider the vibration of a string. The Figure 1 gives us a possible abstract representation of these situations.

A brief study of the problem of free vibrations will be conducted. For this, suppose that a string is set in motion in a plane and let $u(x,t)$ be a function denoting the vertical displacement of the string, with ends $x = 0$ and $x = L$, at point x at the moment t. The initial conditions will be described as position and initial velocity.

Considering the initial value problem presented in (1) and assuming $u(x, 0) = sin(x)$, $h(x) = 0$ and $c = 1$, will be as has the following analytical solution

$$u(x,t) = \frac{sen(x+t) + sen(x-t)}{2} = sen(x)\,cos(t). \tag{37}$$

Therefore, $u(x,t)$ is a sine of amplitude $\mid \cos(t) \mid$, being zero for $t = \frac{\pi}{2} + k\pi$, for all $k \in \mathbb{Z}$.

Assuming that the rope is shifted relative to its Equilibrium position and then looses in the instant $t = 0$ with velocity to vibrate freely, it is expected that the adopted vibration mode will acquire different amplitudes without, however, leaving the amplitude.

Applying a finite difference formulation of seven points in the problem 1 we obtain the following explicit equation for the interior points of the mesh

$$\begin{aligned}
&A_3U_j^{n+1} + A_2U_{j+2}^n + A_1U_{j+1}^n + A_0U_j^n + A_1U_{j-1}^n + A_2U_{j-2}^n + A_3U_j^{n-1} = 0, \text{ em } \ t_0 = 0,\\
&U_j^0 = sen(x_j),\\
&U_j^1 = sen(x_j)\,cos(\Delta t) \text{ em } \ t_1 = \Delta t.
\end{aligned} \tag{38}$$

where U_j^0 and U_j^1 initial conditions of the problem whose coefficients will be obtained by means of the canonical basis and the base of characteristic polynomials.

We made experiments for coefficients obtained by both polynomial bases on the domain $\Omega = [0, \pi]$ featuring mode half-sine, with spatial and temporal steps, respectively, by $h = \pi/5$ and $\Delta t = 0.7h$ stencils for both classic and the other stencil, so that the stability condition is satisfied for both. The times used in each plot were $t_n \in \{0, \Delta t, 2\Delta t, 9\Delta t\}$, and in $t_0 = 0$ is plotted the initial condition. Figure 6 shows the vibration modes obtained for the classical formulations and also by the proposed formulation via characteristic polynomials.

The main advantage of our proposal is the considerable gain of the order of convergence. In addition, the stability condition associated with the latter is less restrictive. Graphically it is also observed that our proposal represents more adequately the solution, as shown in Figure 6.

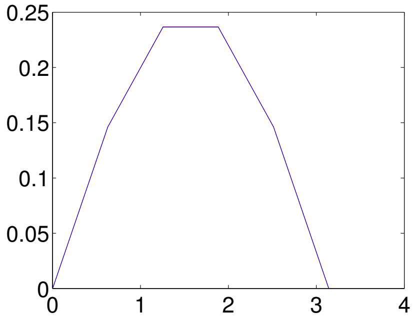

(a) Simulation in $t_0 = 0$

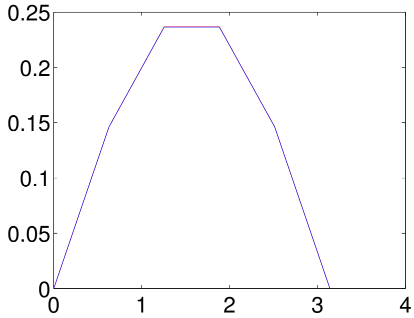

(b) Simulation in $t_0 = 0$

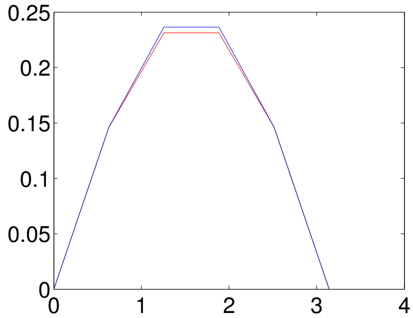

(c) Simulation in $t_1 = \Delta t$

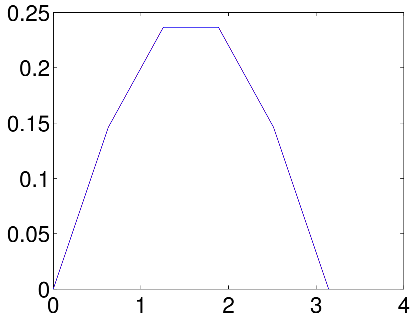

(d) Simulation in $t_1 = \Delta t$

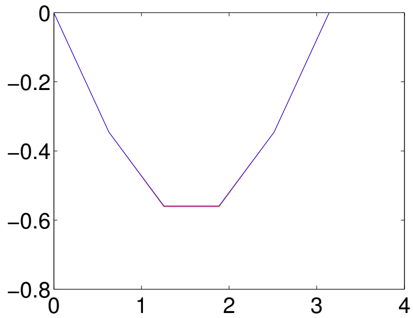

(e) Simulation in $t_4 = 4\Delta t$

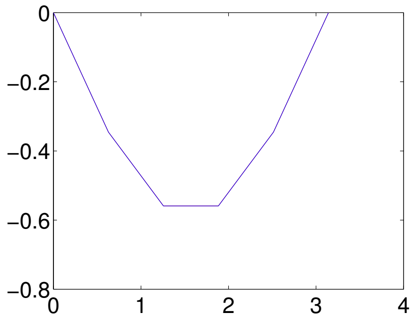

(f) Simulation in $t_4 = 4\Delta t$

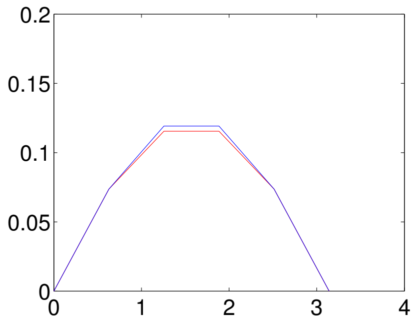

(g) Simulation in $t_{10} = 10\Delta t$

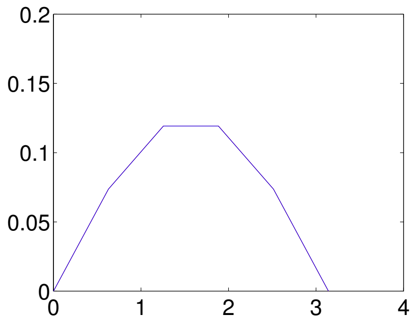

(h) Simulation in $t_{10} = 10\Delta t$

Figure 6: The first column of graphs corresponds to the modes obtained through classical formulation. The second column of images is given by the modes obtained through the polynomial basis of characteristic functions. The exact solution in blue and approximate solution in red.

6.1.1 Numerical verification of the convergence orders

The Table 4 below shows the order of convergence obtained for a stencil of *five* points. As expected from the mathematical analysis, second-order convergence rates were obtained in the maximum norm. We recall both approximations for classical differences and also via characteristic polynomials are equivalent in this case.

$log_{10}(h)$	$log_{10}(emax)$	Convergence rates
0.40594011429780973129	-2.9325238258189935617	$2^{\underline{a}}$ $order$
0.70697010996179092649	-3.6577458259006444765	2.41
1.0080001056257721217	-4.2733813144598147034	2.04
1.3090301012897533169	-4.8838765086862846132	2.03
1.6100600969537345121	-5.4905993671284930004	2.01

Table 4: Convergence of the five-point scheme.

The Table 5 presents, in turn, the order of convergence obtained for a stencil of *seven* points with coefficients obtained via canonical polynomials. Second order rates in the maximum norm were checked in accordance with the orders predicted analytically.

$log_{10}(h)$	$log_{10}(emax)$	Convergence rates
0.40594011429780973129	-2.8199221962043470846	$2^{\underline{a}}$ $order$
0.70697010996179092649	-3.4494561642923876262	2.10
1.0080001056257721217	-4.0400585739661569197	2.00
1.3090301012897533169	-4.6412628176953845329	2.00
1.6100600969537345121	-5.2441052619687071864	2.00

Table 5: Convergence of the classically generated seven-point scheme.

For the seven-point stencil, computational experiments were also carried out in order to obtain results that fit the orders obtained analytically. The table 6 presents the order of convergence of the method obtained for a stencil of *seven* points with coefficients obtained through the base of characteristic polynomials. Where a significant gain of the order of convergence is observed, is a method of fourth order.

$log_{10}(h)$	$log_{10}(emax)$	Convergence rates
0.40594011429780973129	-4.8179449825459891615	$4^{\underline{a}}\ order$
0.70697010996179092649	-6.0601938969701017901	4.1
1.0080001056257721217	-7.2554660271819178916	4.00
1.3090301012897533169	-8.4595278863016978837	4.00
1.6100600969537345121	-9.6647008150439816979	4.00

Table 6: Convergence of the proposed seven-point scheme.

Next, the table 7 presents the order of convergence obtained for a stencil of *nine* points with coefficients obtained classically. As can be seen, the method is of the second order, being compatible with the rates obtained analytically. The Table 8, in turn, exposes the verified convergence order to a *nine* point stencil with coefficients obtained via characteristic polynomials. As can be seen, a sixth order method was generated. Where this convergence rate is in agreement with the analytical mathematical analysis.

$log_{10}(h)$	$log_{10}(emax)$	Convergence rates
0.40594011429780973129	-3.0933415384435719364	$2^{\underline{a}}\ order$
0.70697010996179092649	-3.5065570907297922811	1.40
1.0080001056257721217	-4.0594666942072607880	1.84
1.3090301012897533169	-4.6490080314656674443	2.00
1.6100600969537345121	-5.2475156057945204178	2.00

Table 7: Convergence of the classic nine-point scheme.

$log_{10}(h)$	$log_{10}(emax)$	Convergence rates
0.40594011429780973129	-6.7344783235273342640	$6^{\underline{a}}$ $order$
0.70697010996179092649	-8.3599824994159366248	5.40
1.0080001056257721217	-10.117520066598948368	5.84
1.3090301012897533169	-11.911449386799542332	6.00
1.6100600969537345121	-13.715040597202124895	6.00

Table 8: Convergence of the proposed nine-point scheme.

6.2 Wave Propagation

In this section, we present numerical experiments that illustrate a phenomenon of wave propagation. When we post t as the time, the conversion $\xi = x + ct$ represents a translation of the left coordinate system with velocity c Analogously to the change $\eta = x - ct$, where in this case the translation of the system will be to the right.

It is easy to verify that for $\phi \in C^2(\mathbb{R})$, the function $u(x,t) = \phi(x \pm ct)$ satisfies the one-dimensional wave equation. In particular, let $u(x,t) = sin(x - ct)$. This solution represents a sine wave that moves to the left with constant velocity c. We define the following model problem on a domain $\Omega \subset \mathbb{R}$,

$$\begin{aligned}
&\frac{\partial^2 u}{\partial t^2} - c^2 \frac{\partial^2 u}{\partial x^2} = 0, \ u \in C^2(\Omega), \ \ 0 < x < L, \ \ t > 0, \\
&u(x,0) = sen(x), \\
&\frac{\partial u(x,0)}{\partial t} = -cos(x).
\end{aligned} \tag{39}$$

The discrete equation associated with a non-compact stencil of seven interior points is explicitly given by

$$A_3 U_j^{n+1} + A_2 U_{j+2}^n + A_1 U_{j+1}^n + A_0 U_j^n + A_1 U_{j-1}^n + A_2 U_{j-2}^n + A_3 U_j^{n-1} = 0, \ \text{em } \Omega = [0, 30\pi] \tag{40}$$

and initial conditions on $[2\pi, 4\pi] \subset \Omega$

$$\begin{aligned}
&U_j^0 = sen(x_j), \ \text{em } \ t_0 = 0, \\
&U_j^1 = sen(x_j - \Delta t) \text{ em } \ t_1 = \Delta t.
\end{aligned} \tag{41}$$

Numerical experiments were carried out also with the approximation through characteristic polynomials. In both situations, 600 points were considered Uniformly distributed over Ω and temporal iterations governed by the times $t_n \in \{0, 19.999, 49.998, 59.998, 79.998, 89.997\}$.

Applying the classical coefficients on the explicit approximation 40 with $h = 30\pi/600$ and $\Delta t = 0.6h$ The graphics results presented in Figure 7. Where it is possible to observe propagation sine waves are given by the exact and approximate solution. In t_0 the initial condition modes are given. The transport takes place as expected, from t_1, in a situation where the stability condition is respected, preserving the modes until the moment the wave is reflected after reaching the contour of the domain.

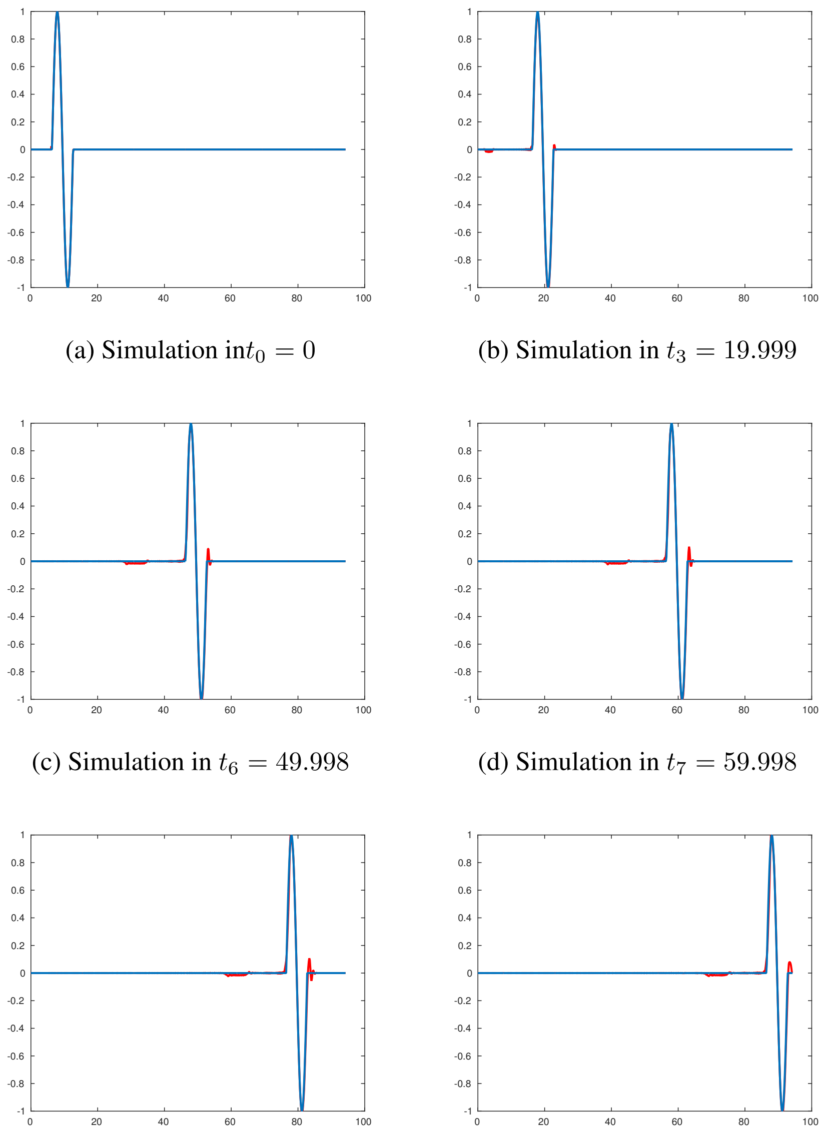

(a) Simulation in$t_0 = 0$

(b) Simulation in $t_3 = 19.999$

(c) Simulation in $t_6 = 49.998$

(d) Simulation in $t_7 = 59.998$

(e) Simulation in $t_9 = 79.998$

(f) Simulation in $t_10 = 89.997$

Figure 7: Transport of the simulated sine wave with mesh parameters $h = 30\pi/600$ and $\Delta t = 0.6h$. Exact solution in blue and solution Approximate in red.

Using now the approximation of finite differences of characteristic polynomials for the seven-point stencil with the same data set from the previous experiment, the results presented in Figure (8)

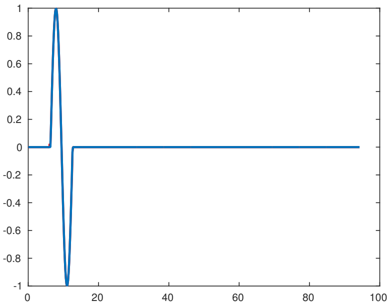

(a) Simulation in $t_0 = 0$

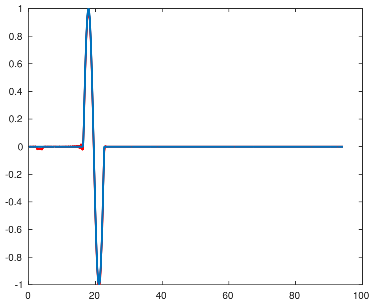

(b) Simulation in $t_3 = 19.999$

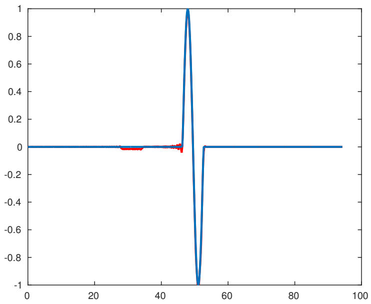

(c) Simulation in $t_6 = 49.998$

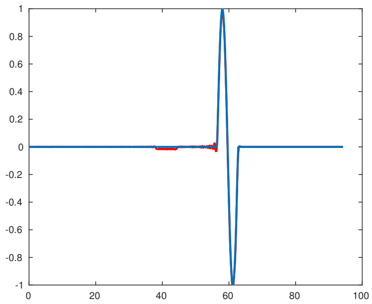

(d) Simulation in $t_7 = 59.998$

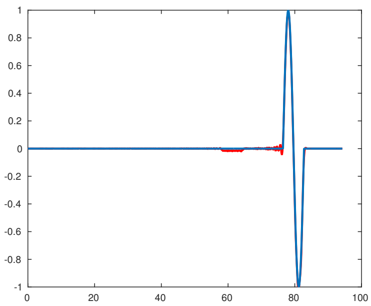

(e) Simulation in $t_9 = 79.998$

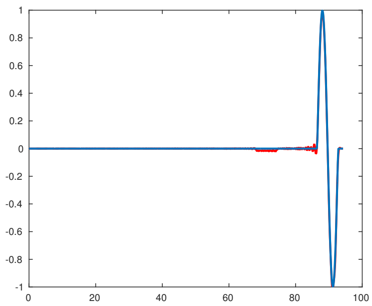

(f) Simulation in $t_{10} = 89.997$

Figure 8: Transport of the simulated sine wave with mesh parameters $h = 30\pi/600$ e $\Delta t = 0.6h$. Exact solution in blue and solution Approximate in red.

Observing the wave propagations classically obtained in the figure 7 and the proposals presented in the figure 8, we notice that our methodology better represents the model problem.

7 CONCLUSIONS

Classically, it is common to use second-order approximations in time and higher orders in space. However, by the condition of stability $\Delta t = O(h)$ the methods are always of second order, since the resulting order is the lowest. We do not use approximations in time or space, we use approximations for the operator, always considering three instants in time and space plus points. Given the way, we construct we generate higher order methods whose order is characterized by spatial discretization. We show that the order of convergence of our proposal is superior to the classical methodologies of finite differences. Numerical experiments were conducted for vibration and wave propagation problems. In addition, we verify numerically the convergence rates obtained analytically.

ACKNOWLEDGEMENTS

The first author thanks the PRH human resources program of the National Agency of Petroleum ANP for the master's degree.

Bibliography

[1] J. D. B. Santos. *Métodos de diferenças finitas de alta ordem para a equação da onda*. Tese de mestrado, LNCC, 2016.

[2] J. D. B. Santos and A. F. D. Loula. Métodos de diferenças finitas de alta ordem para o problema de Helmholtz. *Ibero Latin American Congress on Computational Methods in Engineering*, 2016.

[3] J. D. B. Santos and A. F. D. Loula. Geração de aproximações de diferenças finitas em malhas não uniformes para as edp's de Laplace e Helmholtz. *Proceeding Series of the Brazilian Society of Computational and Applied Mathematics*, 2016.

[4] V. S. Ryaben'kii and S. V. Tsynkov. *A Theoretical Introduction to Numerical Analysis*. Taylor & Francis, 2006.

[5] R. J. LeVeque. *Finite Difference Methods for Differential Equations*. University of Washington, 2005.

[6] T. Liszka and J. Orkisz. The finite difference method at arbitrary irregular grids and its application in applied mechanics. *Computers & Structures*, 11:83–95, 1980.